Creating perfused functional vascular channels using 3D bio-printing technology

Vivian K. Lee [a, b], Diana Y. Kim [a, b], Haygan Ngo [a, b], Young Lee [c], Lan Seo [d], Seung-Schik Yoo [e], Peter A. Vincent [f], Guohao Dai [a, b, *]

[a] Department of Biomedical Engineering, Rensselaer Polytechnic Institute, 110 8th Street, Troy, NY 12180, USA
[b] Center for Biotechnology and Interdisciplinary Studies, Rensselaer Polytechnic Institute, 110 8th Street, Troy, NY 12180, USA
[c] Department of Bio and Brain Engineering, KAIST, Daejeon, Republic of Korea
[d] Department of Biological Sciences, Rensselaer Polytechnic Institute, 110 8th Street, Troy, NY 12180, USA
[e] Department of Radiology, Brigham and Women's Hospital, Harvard Medical School, Boston, MA 02115, USA
[f] Center for Cardiovascular Sciences, Albany Medical College, Albany, NY 12208, USA

ARTICLE INFO

ABSTRACT

We developed a methodology using 3D bio-printing technology to create a functional in vitro vascular channel with perfused open lumen using only cells and biological matrices. The fabricated vasculature has a tight, confluent endothelium lining, presenting barrier function for both plasma protein and high-molecular weight dextran molecule. The fluidic vascular channel is capable of supporting the viability of tissue up to 5 mm in distance at 5 million cells/mL density under the physiological flow condition. In static-cultured vascular channels, active angiogenic sprouting from the vessel surface was observed whereas physiological flow strongly suppressed this process. Gene expression analysis was reported in this study to show the potential of this vessel model in vascular biology research. The methods have great potential in vascularized tissue fabrication using 3D bio-printing technology as the vascular channel is simultaneously created while cells and matrix are printed around the channel in desired 3D patterns. It can also serve as a unique experimental tool for investigating fundamental mechanisms of vascular remodeling with extracellular matrix and maturation process under 3D flow condition.

© 2014 Elsevier Ltd. All rights reserved.

1. Introduction

3D bio-printing, a technology used to construct complex 3D structures via a layer-by-layer approach, has recently been introduced into the field of tissue engineering [1–12]. Compared to traditional 3D printing in manufactory industry, the main features of this technology are using phase-changing hydrogels without harsh chemicals as well as a dispensing technology that is gentle enough for the cells. An important advantage of this technology is its ability to simultaneously deposit live cells, growth factors along with biomaterial scaffolds at precisely controlled locations to mimic the native tissue architecture. The technology has a great potential in tissue engineering, as various functional tissues can be fabricated with appropriate structures and cell compositions in a wide range of sizes, in a high-throughput, and highly reproducible fashion.

Despite this technology's great potential in tissue engineering, several challenges still exist on constructing thick and complex tissues. One of them is the same problem encountered in traditional tissue engineering: the lack of perfused vasculature [13]. Due to diffusion limitation, tissues thicker than a few hundred micrometers have difficulties in survival and proliferation [14]. Building appropriate vascular structure is critical to vitalize thick tissue, and is an important step towards clinical applications of tissue engineering. Previously, we and others have demonstrated that constructing an empty fluidic channel is feasible using 3D bio-printing technology with a sacrificial strategy where the fluidic channel cavity is filled with temporary materials that are subsequently removed [11,15–17].

In this study, we developed 3D bio-printing method to construct a perfused vascular channel within thick collagen scaffold. The vascular channel is constantly perfused and resides on a biologically relevant and porous matrix in which other cell types can be easily introduced to form desired tissue structures during the

---

* Corresponding author. CBIS, Room 3123, Rensselaer Polytechnic Institute, 110 8th Street, Troy, NY 12180, USA. Tel.: +1 518 276 4476.
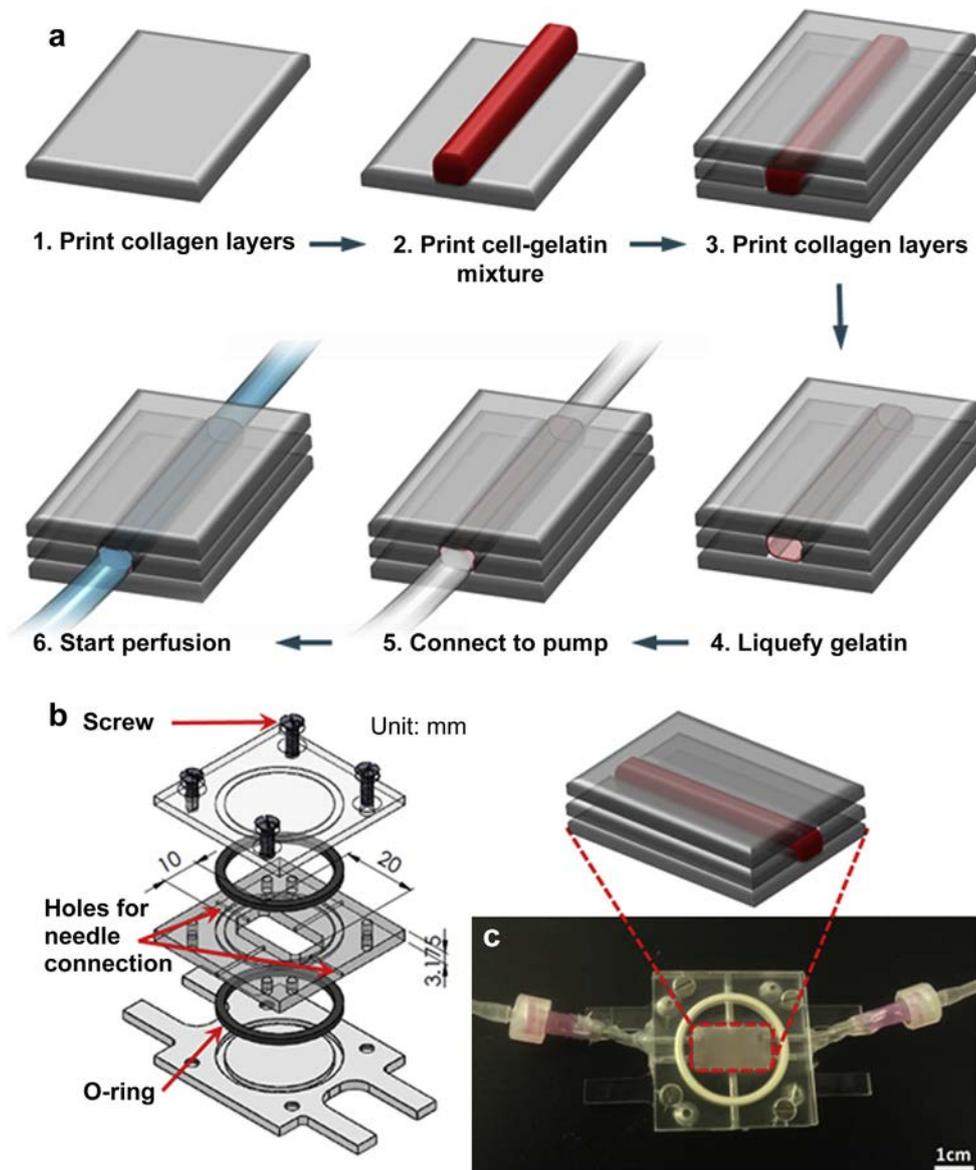E-mail address: daig@rpi.edu (G. Dai).

Fig. 1. (a) Schematics of the vascular channel construction procedure using cell—gelatin mixture. (b) Custom-designed flow chamber consists of three transparent polycarbonate pieces, two o-rings for sealing, and screws. (c) Actual picture of flow chamber. The chamber is connected to the perfusion system through needles installed on the side of chamber.

process of bio-fabrication. For the dynamic tissue culture with physiological shear, we introduced a media perfusion system with a specially-designed flow chamber. The perfusion system was customized for 3D bio-printing applications and guaranteed a stable long-term fluidic culture. Morphological features and barrier functions of the vasculature, and its capability to support tissue viability were assessed. Gene expression analysis was also performed on vascular channels cultured under various conditions. In addition, distinctive cell behaviors in static-cultured vascular channels were reported in this study. Our method of creating the vascular channel provides a way to support the growth and maturation of the bio-fabricated tissue construct, and enhances the capability of the current solid free-form fabrication technology in thick tissue fabrication.

2. Materials and methods

2.1. 3D bio-printing system and printing parameters

We have developed a bio-printing platform based on the 3D solid free-form fabrication technology and demonstrated its capability of printing live cells and biomaterials in previous studies [10—12,18,19]. The printing platform consists of a robotic stage with 3-axis motors, an array of dispenser with microvalves, and an attachable temperature-controlling unit. The liquid-based materials including cell suspensions, soluble chemicals (e.g. growth factors), micro-beads suspension, and hydrogel precursors can be printed while maintaining cell viability. A user-friendly software interface enables on-demand printing of spatial patterns of the materials in 3D at sub-cellular accuracy (~100 μm of resolution for aqueous materials).

The attachable temperature-controlling unit is a cylindrical aluminum casing equipped with thermometers and flexible heaters (Omega Engineering, Inc.). These elements compose a temperature control feedback system, allowing a consistent temperature control during printing procedures. The unit can be directly installed and removed on the microvalve array. Up to 8 separately-controlled units can be installed on the 8-channel dispenser array, allowing simultaneous printing of various thermo-sensitive materials (e.g. gelatin, agarose and matrigel).

In this printing platform, air pressure is applied on the loaded materials and a droplet of the material is dispensed when the microvalve is opened for short time (100—800 μs). The volume of dispensing droplet (i.e. drop size) is adjusted by controlling of valve opening duration and the air pressure. The printing pressure and dispenser valve opening times are crucial parameters for the proper printing of various biomaterial hydrogel and cells. These parameters were determined based upon the viscosity of the biomaterials being dispensed. The lowest pressure that showed stable dispensing without clogging was used for the printing of collagen and gelatin. As 10% gelatin solution at 37 °C is more viscous than collagen precursor, higher pressure was employed for the printing of gelatin compared to collagen. Pressure values in the range of 3.0—4.0 psi and 750 μs for valve opening times were

used for collagen printing. For the printing of gelatin or cell–gelatin mixture, 4.0–5.5 psi of pressure and 750 μs of valve opening time were used.

2.2. Cell culture and hydrogel preparation

Human umbilical vein endothelial cells (HUVECs) were cultured at 37 °C in 5% CO_2 in Endothelial Cell Growth Medium-2 (EGM-2; Lonza). The culture media was changed every two days. HUVECs were routinely passaged onto tissue culture flasks and discarded after 8 passages to ensure representation of key endothelial characteristics. Right before cell printing, cells were harvested using 0.25% Trypsin–EDTA, and then maintained as cell suspensions on ice until ready to be used. To visualize endothelial cells (ECs) by real time imaging, fluorescent-labeled ECs were also generated by transfecting lentivirus expressing eGFP or mCherry (Genecopoeia).

Collagen hydrogel precursor (Rat tail; type I; BD Biosciences) was used as a scaffold material for printing. The collagen precursor from stock was diluted to 3.0 mg/mL using 0.02 N acetic acid and maintained on ice until it was loaded into a syringe (which serves as a printer cartridge) for printing. Gelatin from porcine skin (Sigma–Aldrich) was used as a sacrificial material to create fluidic channels. The concentration of gelatin solution was adjusted to 10%, at which gelatin is reversibly solidified at room temperature and liquefied at 37 °C.

2.3. Flow chamber and perfusion system

In order to provide stable media perfusion for long-term culture, specially-designed polycarbonate flow chambers were fabricated (Fig. 1b, c). The flow chamber consists of three parts (Fig. 1b). The middle part of the flow chamber contains needle holes for luer-connection to the media perfusion system. Before printing, the bottom and middle parts were assembled to provide a container for printed structures. Once printing procedures were finished, the top part was assembled and the flow chamber was connected to the perfusion system.

The perfusion platform includes a digital-control peristaltic pump (Ismatec), a reservoir of culture medium, and the custom-designed flow chamber. Each component is connected to the flow chamber through silicon tubing and polypropylene fittings (Cole–Parmer).

2.4. Construction of vascular channel within thick collagen matrix

Through a layer-by-layer approach, we created a fluidic vascular channel within a 3D collagen matrix using collagen precursor, gelatin, and HUVECs (Fig. 1a). The collagen precursor was printed on a flow chamber (Fig. 1c) and polymerized by NaHCO₃ nebulization [12]. This collagen printing step was repeated 5–6 times to fill the bottom half of the flow chamber (Fig. 1a, step 1). A 1:1 mixture of 20% gelatin and HUVECs (16–20 × 10^6 cells/mL in media suspension) was printed in a straight pattern (Fig. 1a, step 2). The final gelatin concentration and cell density in the mixture were 10% and 8–10 × 10^6 cells/mL, respectively. The gelatin solidified within 1–2 min when it was exposed to room temperature. The flow chamber was kept in 4 °C for 10 min to complete gelatin solidification and to provide a higher degree of rigidity to the gelatin pattern. Then, more collagen layers were printed to cover the gelatin pattern in full (Fig. 1a, step 3). The flow chamber was sealed and incubated at 37 °C for 30–40 min to complete the collagen gelation and conversely, to liquefy the gelatin (Fig. 1a, step 4). During this incubation process, HUVECs captured within the gelatin sank down slowly and attached to the inner surface of the channel. We flipped over the flow chamber every 10–15 min to allow cells to attach to both bottom and top surfaces of the channel. Following this step, the flow chamber was connected to a dispensing pump and gentle media flow (~0.3 mL/min) was applied to wash out the gelatin and to obtain a perfused vascular channel (Fig. 1a, steps 5–6). For the channel samples for dynamic culture, flow rate was gradually increased until it reached 10–15 dyn/cm² of shear stress. Flow rate calculation was based on channel dimensions. 1.5–4.0 mL/min of flow was applied, depending on channel dimensions. Culture media was changed every other day. For samples undergoing static culture, the channel was disconnected after washing out the gelatin; then, media was manually changed every day. EGM-2 with 2% dextran (~500 kDa, Sigma, media viscosity: 0.02 P) was used for both static and flow conditions.

A variation of this construction method was also developed. In this method, an empty channel was created using gelatin only, without cell suspensions. After liquefying the gelatin, HUVECs (8 × 10^6 cells/mL in media suspension) were next seeded in the channel by injecting cell suspension into the empty channel and incubating for 1 h. During the cell seeding, we flipped over the flow chamber every 10–15 min to allow cells to attach to both bottom and top surfaces of the empty channel. The original channel fabricating method caused a minor cell death due to the gelatin encapsulation (~90% of viability). Thus, higher cell density was required for this procedure. The second method guaranteed a higher cell viability (>95%) and thus required less number of cells. However, after several days of culture, there was no significant difference in the cell viability and the morphology and function of the vascular channels made by the two different methods. Although the second method has its advantage on cell viability at the beginning of the culture period, we pursued the original method because of the following reasons: a) additional seeding step (Fig. 1, between steps 4 & 5) was not required, and b) this technique provides greater flexibility when dealing with more complicated vessel patterning.

2.5. 2D flow set-up

To compare the influence of flow on gene expression in 2D and 3D culture conditions, 2D flow experiments was performed on a confluent monolayer of HUVECs using an ibidi μ-slide (ibidi GmbH). The ibidi μ-slide was coated with 0.1% gelatin solution for 1 h before cell seeding. HUVEC suspension (4 million cells/mL) was injected into the ibidi slide and incubated for 1 h. After seeding, half of the sample set was connected to flow systems and cultured for 5 days with 10 dyn/cm² of flow. Culture media were changed every other day for the flow samples. The other half of the sample set was cultured in a static condition for 5 days with a media change every day.

2.6. Viability analysis

In order to assess the capability of the vascular channel to support adjacent tissue viability, different densities of ECs were printed nearby the vascular channel (1, 5, and 55.8 million cells/mL) to create tissue structure with various cell densities. In other words, the samples prepared for viability test consisted of two components: 1) a vascular channel (seeding density: 8 million cells/ml); and 2) outer collagen matrix with embedded endothelial cells (seeding density: 1, 5, or 55.8 million cells/ml). The only difference between this viability test sample and the single channel sample (described in Section 2.4) was whether additional cells were embedded within collagen matrix. In both experiments, the cell seeding density used to create vascular channel was identical, 8 million cells/ml. The printed tissue constructs were cultured for 3 days either in the static condition or the flow condition. For the tissues cultured in the static condition, media were changed every day. At the end of the culture period, old media were replaced with fresh media containing reagents from the Live/Dead Viability kit (Invitrogen; green-fluorescent calcein-AM to indicate intracellular esterase activity and red-fluorescent ethidium homodimer-1 to indicate loss of plasma membrane integrity), and incubated for 3 h. Following incubation, the samples were washed with fresh media. They were then imaged using a wide-field fluorescent microscope (Nikon Ti). The images were collected as z-stacks and then compressed onto a single plane by maximum intensity projection.

2.7. Measurement of diffusional permeability

To assess barrier function of the printed vascular structure, diffusional permeability of the vascular channel was assessed by injecting culture media containing 50 μg/mL Alexa Fluor 488-conjugated bovine serum albumin (BSA; Invitrogen) or 20 μg/mL Alexa Fluor 594-conjugated 10 kDa dextran (Invitrogen). Diffusion pattern of each molecule was detected by using different fluorescent filters of wide-field microscope (Eclipse Ti, Nikon). BSA diffusion was visualized in green color using B-2E/C filter (λ_{ex} = 480 nm, λ_{em} = 535 nm), and dextran diffusion was visualized in red color using G-2E/C filter (λ_{ex} = 540 nm, λ_{em} = 620 nm). After injection, fluorescence images were captured every 2 min for 30 min using a wide-field fluorescent microscope. A diffusional permeability of each molecule was separately calculated by quantifying changes of fluorescent intensity over time using the following equation;

$$P_d = \frac{1}{I_1 - I_b}\left(\frac{I_2 - I_1}{\Delta t}\right)\cdot\frac{d}{4},$$

where P_d is diffusional permeability coefficient, I_1 is average intensity at an initial time point, I_2 is average intensity after delta time (Δt), I_b is background intensity, and d is diameter of the channel [20]. The permeability measurement was performed on a total of four types of channel structure: 1) Flow-cultured channel with cell lining, 2) Flow-cultured channel without cell lining (empty channel), 3) Static-cultured channel with cell lining, and 4) Static-cultured channel without cell lining (empty channel). For each type, the diffusional permeability was calculated from the measurement of four samples ($n = 4$).

2.8. RNA isolation and real-time PCR

RNA was isolated by using QIAzol lysis reagent (Qiagen) and treated with DNase (Invitrogen) according to the manufacturer's protocol. The concentration and quality of RNA were determined by NanoDrop (NanoDrop Technologies). RNA was isolated from a total of four types of experimental conditions: 1) HUVECs cultured on tissue culture plate (2D static), 2) cells cultured in the ibidi channels under the flow condition (2D flow), 3) cells cultured in the collagen vascular channels in static condition (3D static), and 4) flow condition (3D flow). Real-time PCR reactions were performed using commercially available TaqMan RT-PCR assays (Life Technologies). For each type, RNA was isolated from four independent experiments ($n = 4$). Gene expression level of each sample was separately measured and analyzed. p Value was obtained from t-test. For any given gene, the regulation was considered as statistically significant when $p < 0.05$.

2.9. Immunostaining and cryosectioning

Following the five days of dynamic culture, the vasculature channels were fixed with 4% paraformaldehyde. The immunostaining of VE-Cadherin (vascular endothelial cadherin) marker was performed using Mouse Anti-Human Cadherin-5 antibody (BD Transduction Laboratories™) and Alexa Fluor 488 Goat Anti-Mouse IgG (H + L) antibody (Life Technologies) to visualize the morphology of individual HUVECs that forms vascular channels. Each antibody incubation step was followed

by three washing steps with DPBS at 10 min each. For the cross-sectional images, several channel samples were embedded in optimal cutting temperature compound (Andwin Scientific), frozen using dry ice, and sectioned using a microtome into 10 μm-thick slices.

2.10. Beads injection

In order to visualize the flow pattern, green fluorescent beads (0.2 μm; Bangs Laboratories, Inc.) were added to the culture media (Fig. 2b). The media containing green beads was perfused with 10–15 dyn/cm^2 of flow rate, and the beads flow pattern was imaged using a wide-field fluorescent microscope. To verify the existence of luminal structure in angiogenic sprouts, 10 μm size of FluoSpheres® Polystyrene Microspheres (Invitrogen) were injected into the vascular channel through the luer-connection (Fig. 4g).

3. Results

3.1. Construction of vascular channel

A single vascular channel was successfully created within a 3 mm thick collagen I scaffold. With the printing parameters

described above (4.0–5.5 psi of pressure and 750 μs of valve opening time for gelatin printing), the dimension of constructed fluidic channels was in the range of 0.7–1.5 mm for the width and 0.5–1.2 mm for the height (Fig. 2a–d). The channel has elliptical shape of cross-section due to the nature of droplet formation by inkjet printing (Fig. 2d). The media flow pattern was verified by injection of green fluorescent beads into the vascular channels (Fig. 2b). The disconnection of the flow pattern was due to the stitching of multiple images. A straight laminar flow was observed under media perfusion condition (10–15 dyn/cm^2 of flow rate) without any leakage of 0.2 μm micro-beads, showing that the printed channel supported non-leaking perfusion under a physiological laminar flow condition. The structural integrity of the vascular channel was maintained under the flow condition for up to three weeks (data not shown). HUVECs covered 70–80% of the inner surface area of the fluidic channel on Day 0. The cells proliferated and covered the entire inner surface within 2–3 days of dynamic culture. The immunostaining of VE-cadherin showed
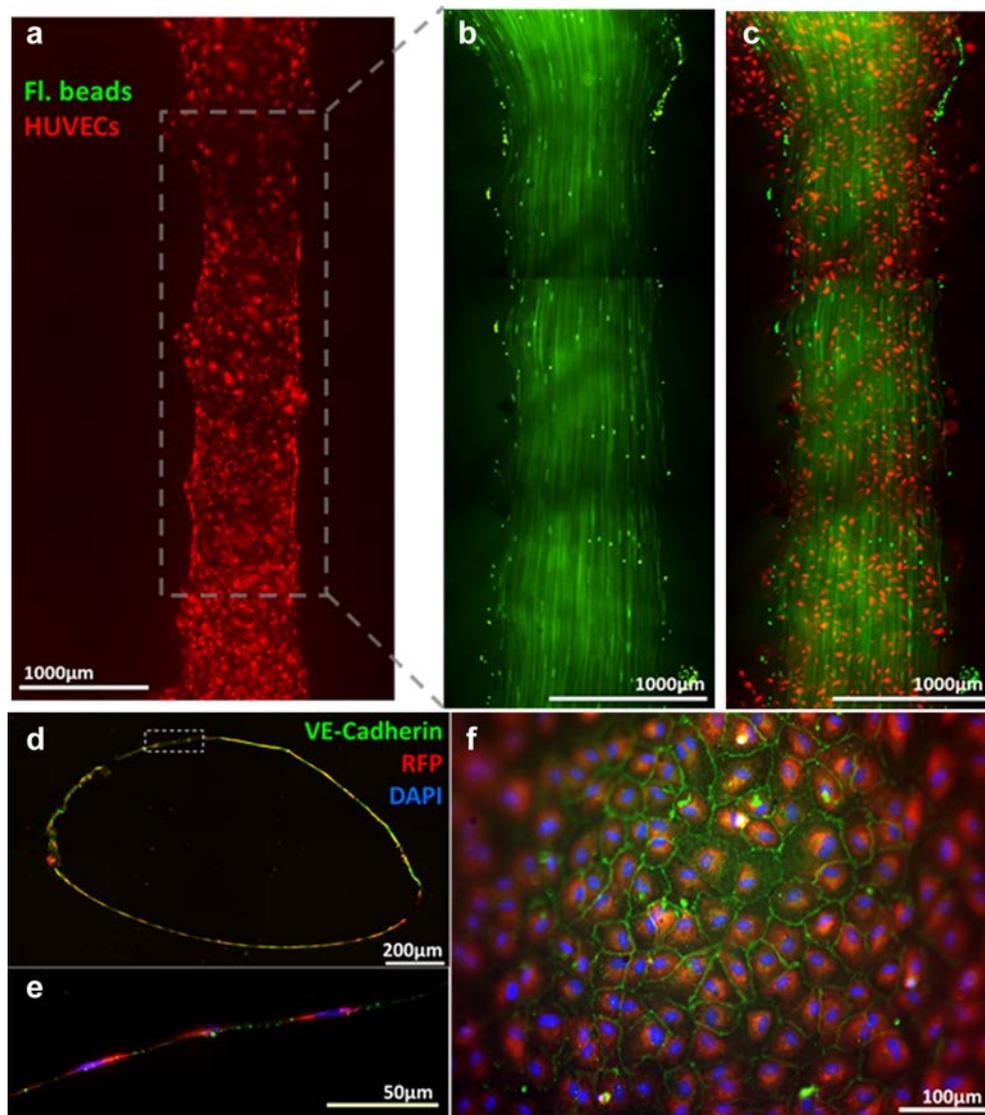

Fig. 2. (a) Fluorescent images of vascular channel system on Day 1 of dynamic flow culture. Large image of endothelial cells (red) seeded on the printed channel. (b) Laminar flow in the vascular channel was visualized by motion of green fluorescent beads. Discontinuity of flow pattern is due to stitching (mosaic) of multiple images. (c) Overlay image of the flow of green beads and printed endothelial cells. (d) Cross-section of vascular channel after 5 days of dynamic culture. (e) Magnification of dotted inset area in (d). Endothelial cells formed a monolayer along the inner surface of the channel. (f) Fluorescent image of inner surface of vascular channel after 5 days of dynamic culture. The edge of the image is out of focus due to a curved surface of the channel. (d–f) blue: DAPI nuclei staining; red: RFP-transfected HUVEC; green: VE-cadherin. (For interpretation of the references to color in this figure legend, the reader is referred to the web version of this article.)
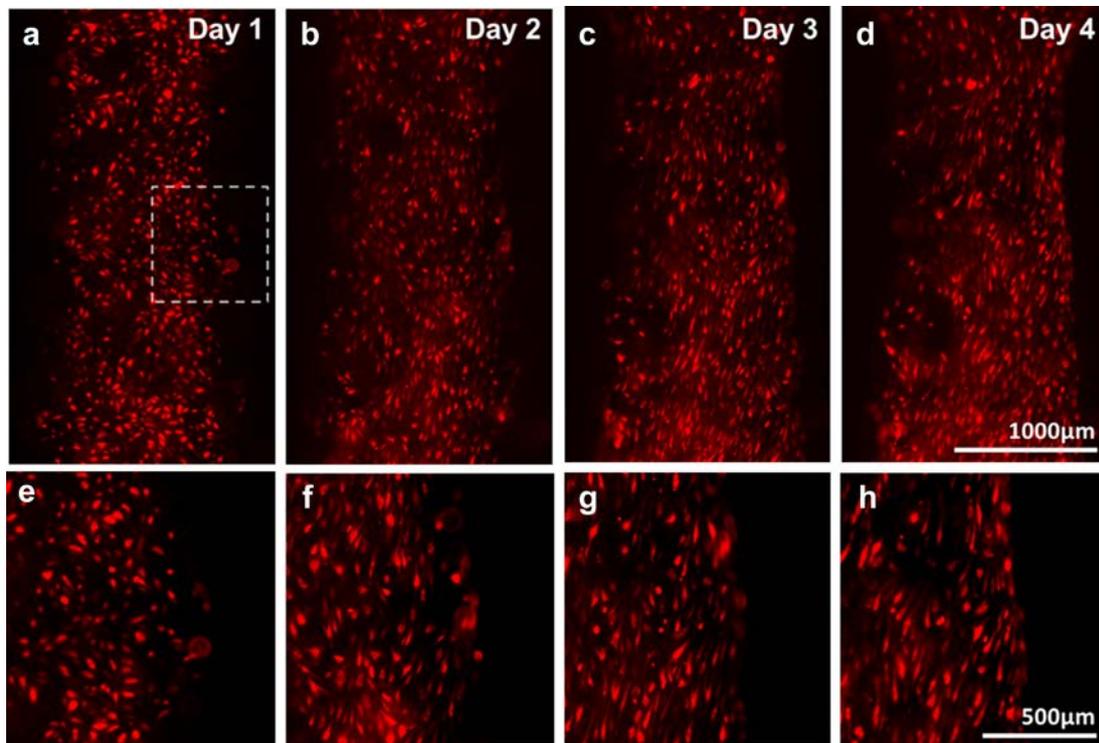
Fig. 3. (a–d) Alignment of HUVECs and change in channel edge shape over the dynamic culture period (Days 1–4). HUVECs were elongated in the direction of flow (flow from top to bottom). The edge of channel straightened. (e–h) Magnification of dotted inset area in (a–d).

that the confluent HUVEC monolayer formed adherence junctions on Day 5 (Fig. 2e, f).

Under the flow culture condition, HUVECs on the channel edge were elongated and aligned along the flow direction (top to bottom) over time (Fig. 3). We also observed endothelium remodeled the surrounding matrix and a straightening on the edge of the vascular channel over time (Fig. 3). The printed channel has an uneven edge shape due to the mechanism of inkjet printing, in which multiple droplets are merged to create a pattern. As the cells were elongated by shear over the culture period, the uneven edge of channel became smoother and straightened. HUVECs in the channel stayed on the channel surface under the flow condition. No invasion of cells into the collagen scaffold was observed for up to two weeks of flow culture.

3.2. Endothelial cell behavior under flow vs. static condition

Along with the flow culture, a static culture condition was applied on several vascular channels. Among multiple differences between the flow- and static-cultured channels, the cell behavior on the channel edge was the most distinctive. As mentioned above, the channels under the dynamic culture condition experienced an endothelium straightening and the cell elongation, and all the cells stayed inside of the fluidic channel (Figs. 3 and 4a, c). On the other hand, HUVECs cultured in the static condition escaped from the channel edge, actively invading into the collagen scaffold and forming angiogenic sprouts (Fig. 4b). The sprouting initiated on Days 3–4 all over on the channel edge, and extended up to 400 μm on Day 7 (Fig. 4e–g). As the sprouts continued to invade and extend into the collagen matrix, they became longer, contained progressively more cells, and began to branch. Stereotypical sprouting morphology was observed in these sprouts, presenting thin filopodia-like protrusions at the sprout tips (Fig. 4d). In most of the cases, cell migration into the collagen matrix was exclusively

occurred by angiogenic invasion and sprouting. Single cell migration into the matrix was rarely observed. Luminal structure was developed in these sprouts, and the existence of lumen was confirmed by injecting fluorescent microbeads (Fig. 4h). These 10 μm size of red fluorescent beads filled the root and stalk part of the sprouts, presenting the luminal structure with >10 μm of diameter.

In contrast, the proliferation of HUVECs was suppressed under the flow condition. The optimized seeding density of HUVECs was 8 million cells/mL. With this cell density, the inner surface of the channel was 70–80% covered on Day 0 (right after channel fabrication) and fully covered within 2–3 days under the flow condition. In the case of static-cultured channel, the inner surface was fully covered within a day. When we used lower seeding density (4 million cells/mL), HUVECs cultured on the static channel proliferated and fully covered the surface in 5 days of culture. In the same condition of cell density, the flow-cultured channel required two weeks to fully cover the entire inner surface area (data not shown).

3.3. Capability of supporting tissue viability

In order to assess the capability of the vascular channel to support adjacent tissue viability, we fabricated multiple vascular tissues with different cell densities. Fig. 5 shows the result of viability assay on the tissues after 3–4 days of static or flow culture. A considerable amount of cell death was observed in the vascular tissue construct cultured in static condition (viability: <10%, Fig. 5a), whereas most of the cells were alive in the tissue within 5 mm of distance to the channel with cell density of 1 million cells/mL or 5 million cells/mL density (viability: >90%, Fig. 5b, c). However, in a vascular tissue with higher cell density (55.8 million cells/mL in this study), cells located more than 400 μm apart from the channel were mostly dead after 4 days, even with 10 dyn/cm^2 of media perfusion (Fig. 5d).
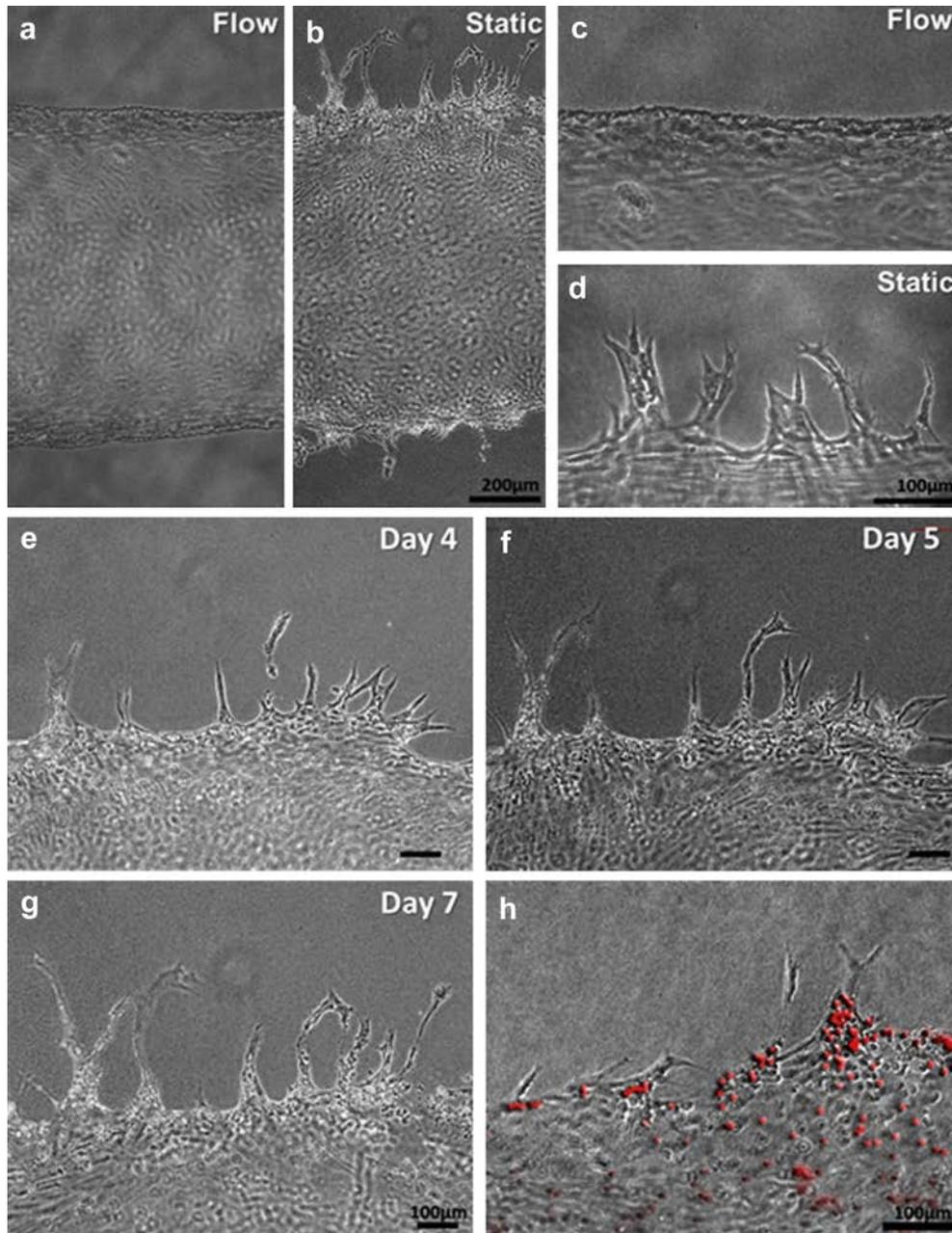
Fig. 4. Morphology of HUVECs on the vascular channel edge in dynamic culture (a, c) and static culture (b, d) on Day 5. (e–g) In the static condition, the sprouts budded from the channel edge extended over culture time, maintaining filopodia-like protrusion on the tip of the sprouts. (h) Luminal structure of sprouts was confirmed by the injection of fluorescence microbeads (10 μm).

3.4. Barrier function characterization

In order to characterize the barrier function of the vascular channels, bovine serum albumin (BSA) and 10 kDa dextran were co-injected into the vascular channel with the flow rate of 10 dyn/cm^2. BSA is a plasma protein, predominantly transported via transcellular pathway. Whereas, dextran is a polysaccharide molecule with various molecular weight, transported around individual ECs via paracellular pathway [21].

Because it is difficult to obtain depth-resolved images in thick tissue using the current image technique, signal intensity was acquired by wide-field fluorescent imaging. This leads to the signals that come from all depth of the tissue instead of just the focal plane. Therefore, fluorescent molecules that diffuse into z-direction will appear brighter in the images. Due to the limitations in 3D imaging, the diffusion pattern of cylindrical structure shows a sinusoidal profile of fluorescence, and the higher intraluminal fluorescence intensity represents the higher diffusion rate. In an empty channel without cell lining, a sinusoidal profile of fluorescence was observed due to the structural characteristic of the cylinder-shaped channel (Fig. 6f). The slope of line plot was decreasing over time, indicating a temporal diffusion from the channel into the bulk gel (Fig. 6f). This diffusion pattern is indicated as blue lines in Fig. 6d and e. In a vascular channel with EC lining cultured under flow condition for 5 days, BSA was gradually concentrated on the lumen surface and perivascular area (Fig. 6a). This BSA accumulation was indicated as two peaks near the channel edge area (Fig. 6d, arrows). We also observed that the signal intensity in the luminal space without EC
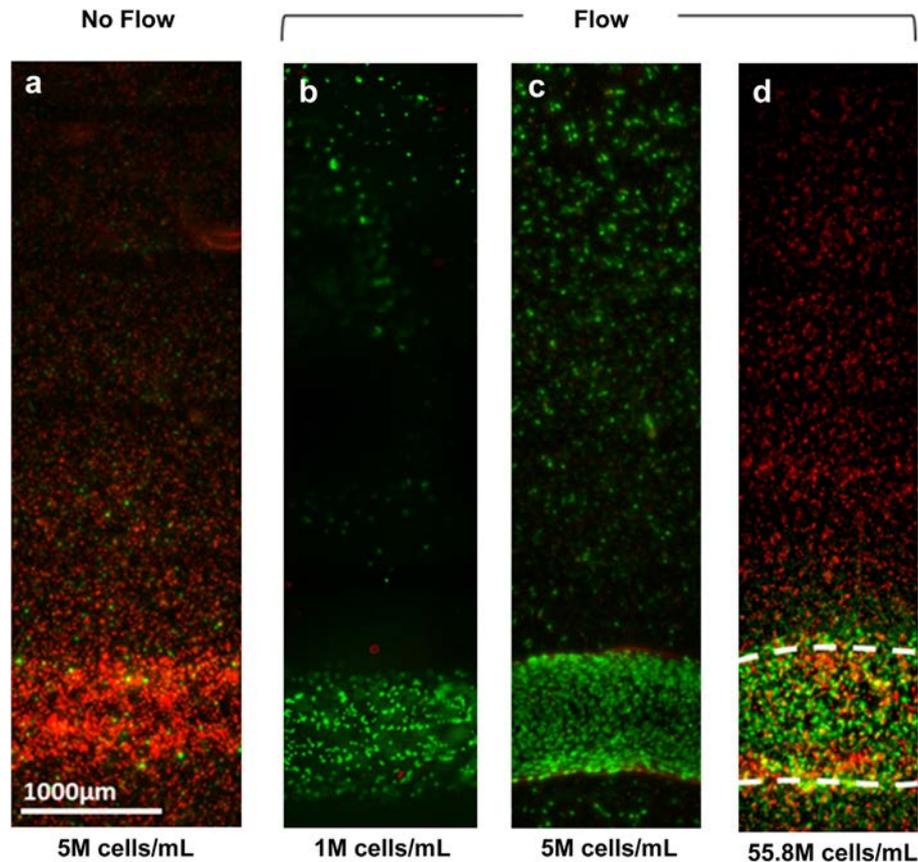
Fig. 5. Viability assay of 3D vascular tissue. 3D vascular tissues with different cell densities were fabricated, culture for 3 days, and labeled with green (live) and red (dead) fluorescence. (a) A considerable amount of cell death was observed in the vascular tissue construct cultured in static condition (viability: <10%). (b–c) With the media perfusion in physiological flow rate, >90% of cells were alive in the tissue with cell density of 1 million cells/mL (b) or 5 million cells/mL density (c). (d) In a vascular tissue with cell density of 55.8 million cells/mL, cells located more than 400 μm apart from channels were dead after 4 days, even with perfusion. (For interpretation of the references to color in this figure legend, the reader is referred to the web version of this article.)

lining is significantly higher than that of channel with EC lining, whereas the intensity in the outer collagen scaffold is similar in both cases. The result implies an active transportation of BSA across the endothelium. In the permeability assay of 10 kDa dextran, no molecule accumulation on the lumen surface was observed (Fig. 6b). However, minor delay of diffusion was found in intensity profile (Fig. 6e, flat area near the channel edge). The signal intensity of dextran in the luminal space is also significantly lower than that of empty channel. Unlike BSA profile, which shows similar level of intensity on the channel edge and in the middle of channel (Fig. 6d), overall shape of dextran profile maintained sinusoidal profile except the minor decrease of slope on the lumen edge (Fig. 6e).

The same permeability assay was performed on vascular channels cultured in static condition for 5 days. Similar BSA accumulation and BSA/dextran diffusion profile were observed in static samples (data not shown). The diffusional permeability was calculated by quantification of fluorescent intensity and presented in Fig. 6c. The calculation result shows that diffusional permeability is about twice higher in an empty channel than a channel with cell lining. However, due to the extensive light scattering and the limitation of the imaging techniques in thick tissue as well as the sample variability, statistically significant difference was not detected.

3.5. RNA expression analysis

To assess the potential of this vessel model in vascular biology research, we performed RT-PCR analysis on several EC gene expression related to vasomotor/thrombosis and arterial/venous identities. RNA was isolated from the four sample sets (2D static, 2D flow, 3D static, and 3D flow) after 5 days of culture, and the RNA expression was measured by RT-PCR (Fig. 7). KLF2 (Krüppel-like Factor 2) was significantly up-regulated by chronic laminar flow in both 2D and 3D conditions, as described in previous studies [22–24]. Connexin40 was strongly induced in 2D flow condition but not in 3D condition. eNOS (Endothelial nitric oxide synthase), HEY1 (Hairy/ enhancer-of-split related with YRPW motif protein 1), Ephrin-B2 also showed an increasing tendency with flow. Interestingly, ECs in the vascular channel show distinct response to flow condition in comparison to those in 2D condition. tPA (Tissue plasminogen activator) is an anti-thrombotic mediator and has been known to increase after exposure to laminar flow for 24 h [25]. However, in our experiments, tPA expression was down-regulated in 2D flow but up-regulated in 3D flow condition when ECs were chronically exposed to flow for 5 days. PCNA (proliferating cell nuclear antigen) expression was reduced in flow and also in 3D condition, confirming our observation that cells grow slower in 3D channel and flow. In 3D static condition, three arterial markers were down-regulated (HEY1, Ephrin-B2, and DLL4) compared to control, then increased after exposed to flow. Other arterial markers (Connexin40, Jagged1, Nrp1) and venous markers (COUP-TFII, Nrp2 and EphB4) showed very little response to flow condition when they are in 3D environment.

4. Discussion

Using the 3D bio-printing technology, we created perfused functional vascular channels. The vascular channel had a lumen
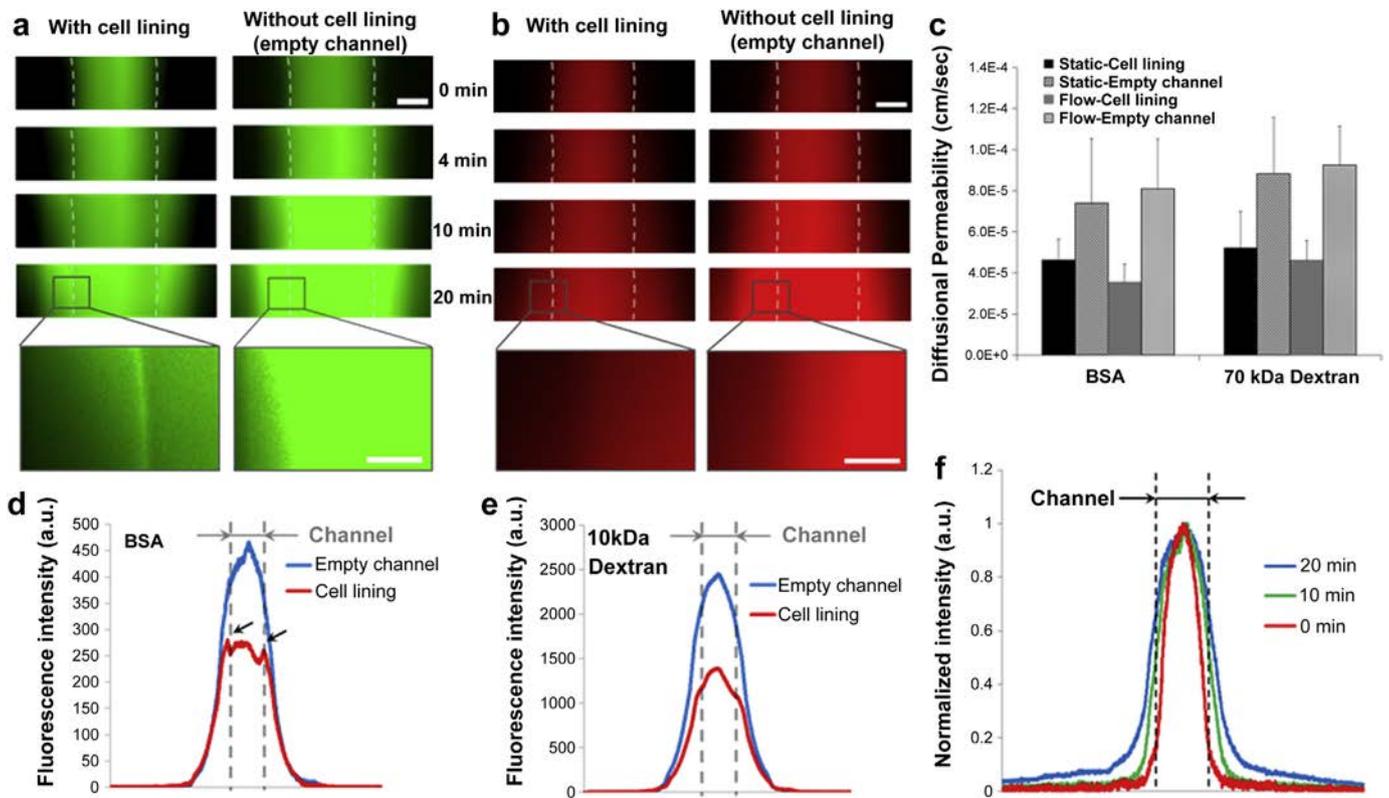
Fig. 6. Time-lapse fluorescence images of (a) BSA (green color) and (b) 10 kDa dextran (red color). (c) Diffusional permeability calculation of BSA and dextran. Scale bar: 500 μm. Scale bar in the magnified inset: 150 μm. (d, e) Line plots of fluorescence across the collagen scaffold and channel after 20 min of perfusion with (d) BSA and (e) dextran. The position of vascular channel is indicated with gray dotted line. (f) Line plot of normalized fluorescence across the collagen scaffold and channel (indicated with black dotted line). (For interpretation of the references to color in this figure legend, the reader is referred to the web version of this article.)

structure covered with confluent EC monolayer, and the structure was maintained for up to two weeks of dynamic culture with physiological shear condition. The fluidic channel supported the viability of adjacent tissue and showed barrier function for a plasma protein and high-molecular weight dextran molecules.

The printing procedure guarantees high cell viability (~90%). The major cause of cell death seemed to be the gelatin encapsulation, as

the viability decreased when higher concentration of gelatin was used or the incubation time for gelatin liquefying (Fig. 1a, step 4) was longer. However, 90% of cell viability was sufficient to create the vascular channel. The constructed fluidic channels have an elliptical shape of cross-section due to the nature of inkjet printing mechanism. When a dispensed droplet hit the substrate, it spread out slightly and formed a flattened hemisphere. Thus, the cross-
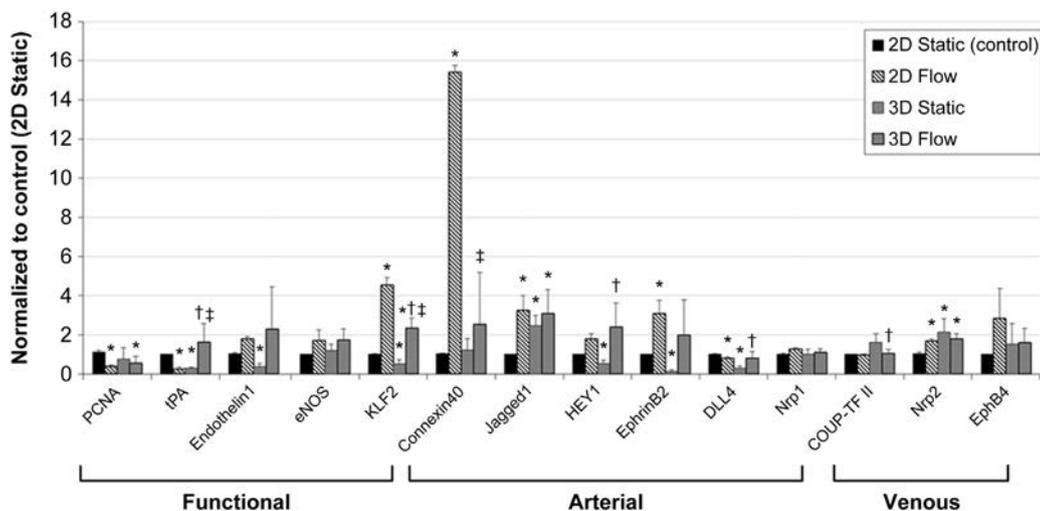

Fig. 7. RNA expression of HUVECs culture in 2D static, 2D flow, 3D static, and 3D flow condition. RNA expression was measured by TaqMan RT-PCR ($n = 4$) on Day 5. All data are normalized to the control condition (2D static, cultured on tissue culture plate). *$p < 0.05$, compared with 2D static (control). †$p < 0.05$, compared with 3D static. ‡$p < 0.05$, compared with 2D flow.

section of printed channels is oval-shaped as shown in Fig. 2d. With the printing parameters described above, the dimension of the fluidic channel had a wide range (0.7–1.5 mm for the width and 0.5–1.2 mm for the height). This could be due to the variation of air pressure applied on the gelatin or cell–gelatin mixture (range of 4.0–5.5 psi). Humidity, minor variance in the gelatin viscosity, and the dispenser condition can also influence the channel diameter and structures. The dimension can be further adjusted by altering printing parameters (e.g. air pressure, valve opening time, and droplet spacing) and by repetitive printing of a gelatin pattern (repeating step 2 in Fig. 1). The printing parameters (air pressure and valve opening time) mainly influence the width of the channel, whereas the sequential number of printing has a higher impact on the channel height.

The vascular channel maintained its structural integrity for long-term tissue culture under the flow condition. No leakage, flow turbulence, or shrinking of scaffold material was observed for up to two weeks of dynamic culture. Under the flow culture condition, HUVECs on the channel edge were elongated and aligned along the flow direction (top to bottom) over time (Fig. 3). This is an important adaptive mechanism that alters the way that shear acts on the cytoskeleton [26]. Also, the uneven edge of channel straightens with the flow culture, which seems to be a result of ECM remodeling during lumen morphogenesis [27–29].

In the static-cultured vascular channels, we observed very distinctive cell behaviors and tissue development. Angiogenic cell invasions actively occurred on the vascular channels, forming sprouts with lumen structures (Fig. 4). Although no chemotactic gradient (e.g. gradients of proangiogenic factors) was applied within the whole collagen construct, the majority of sprouts grew in the orthogonal direction of the channel edge. The morphology of sprouts budded from the channel is comparable to other 3D angiogenesis studies, in which ECs from endothelium-coated surfaces formed angiogenic sprouts towards to the 3D matrices [30,31]. However, there is difference in the initiation time point, growth rate, and branching pattern, mostly due to variance in gel concentration and composition, and difference in culture media ingredients. The luminal structure on the root and stalk part, thin filopodia-like protrusions at the sprout tip, and branches/bifurcations were observed in our model, showing morphological features of developing and matured capillaries [32,33]. In addition to the vessel sprouting, we found that the proliferation of HUVECs was suppressed under the flow condition. The results correspond with previous studies that reported a long-term exposure of the endothelium to shear inhibits cell proliferation and lowers the metabolic rate [34].

When there were no cells embedded within the matrix, viability of endothelial cells seeded on the vascular channel can be supported by changing culture media every day (Fig. 4, static samples). However, when additional ECs were embedded within the matrix around channel, a considerable amount of cell death was observed in the vascular channel (Fig. 5a). This cell death may be due to an increase consumption of oxygen and nutrients caused by the large number of surrounding cells. Similar cell death in the vascular channel was observed in flow-cultured structure with 55.8 million cells/ml (Fig. 5d). Although culture media was consistently supplied, there was a limitation on maintaining cell viability of vascular channel probably because of high oxygen/nutrient consumption when large number of cells was embedded nearby the channel. Considering that the tissue viability was successfully supported in the samples with lower cell density (Fig. 5b, c), the collagen matrix allows transportation of nutrient and oxygen. The diffusion pattern of BSA and dextran was shown in Fig. 6, confirming the molecular transportation through the thick collagen matrix.

The test result of tissue viability indicates that, in a simple tissue model with low cell density ($<5 \times 10^6$ cells/mL), cell viability can be achieved by providing fluidic channels spacing at millimeter scale within the tissue construct. However, for more complex and dense tissue with high cell density (in the order of 10^7–10^8 cells/mL), a denser vascular system (e.g. capillary network) is required to support the cell viability during tissue growth and maturation process. Our 3D bio-printing platform is able to create vascular channels of 500 μm at a distance of 700 μm between multiple channels, which is still far from the density of the capillary network seen in vivo. However, the technology provides a path to address the viability issues in a thick, dense, and complicated tissue by introducing supporting mural cells with ECs and inducing angiogenesis/vasculogenesis within the tissue structure [35–37].

In the barrier function test, a significant BSA accumulation was observed on the lumen surface and perivascular area, and the signal intensity in the luminal space is considerably lower than that of an empty channel (Fig. 6a). The result indicates transvascular transportation of plasma protein [21,38,39]. In the case of 10 kDa dextran, no molecule accumulation on the lumen surface was observed (Fig. 6b), however, minor delay of diffusion was found in intensity profile (Fig. 6e, flat area near the channel edge). The results showed that the channel is functioning as a physical barrier for the passive diffusion of dextran molecules. In this study, the diffusional permeability was calculated based on the changing of fluorescent intensity in the observation window. However, the formula to calculate the diffusional permeability is mostly determined by how fast the molecules diffuse within the collagen gel whereas less on how it across the endothelial barriers. Thus, it is not a surprise that we did not reach statistically significant difference between samples with and without EC lining, since the molecular diffusion within the collagen matrix are the same in both cases. In addition, there are significant limitations on measurement methods for thick and translucence scaffold materials inside of sealed plastic flow chambers, especially with out-of-focus signals from scattered light in collagen gel. Thus, actual filtration parameter across the vessel membrane was not characterized in this study, although the diffusional permeability patterns relatively presents the distinction between the endothelium and the empty channel. An improved imaging technique capable of measuring the depth-resolved signal intensity in large scale in real time is essential to address the limitations. Mesoscopic fluorescence molecular tomography [11,19] capable of imaging depth-resolved fluorescent signals in thick 3D structure is currently under development to improve its sensitivity and imaging performance, and can be served as an imaging tool to evaluate an actual filtration of molecules across the endothelium.

We have demonstrated the capability of the bio-printed vascular channel for gene expression analysis. Although several in vitro technologies were introduced to create vasculatures within matrices with appropriate perfusion system [16,29,40,41], most of the studies rely on immunostaining for further investigation of vascular biology in their vascular structures due to the limitation on cell numbers and gene isolation techniques. The single vascular channel fabricated in this study typically contains 10,000–20,000 cells, sufficient enough for high quality RNA isolation and reliable gene expression analysis. In this model, the ECs reside on a biologically relevant porous matrix and are constantly perfused, thus allowing us to investigate the influence of physical parameters (e.g. matrix stiffness, transmural pressure between lumen and the matrix) on EC functions, which are otherwise difficult to achieve with current 2-D flow models. Our data demonstrated that ECs cultured in the 3D matrix have distinct response to hemodynamic stimuli compared to those on 2-D plastic surfaces. We found that flow induced expression patterns are similar for some genes (e.g. KLF2). However, for selected genes, the expression patterns are different. For example, tPA was reduced in

the 2D condition when ECs were chronically exposed to flow whereas it was increased in the 3D flow condition. On the other hand, Connexin40 was strongly up-regulated in the 2D flow but showed little change in the 3D condition. Overall, we found very little change in the arterial and venous markers in response to the 3D flow condition. Recent studies have found that, when a vein graft undergoes arterialization, venous markers (EphB4) get lost while arterial markers (Ephrin-B2, DLL4, Notch4) are not gained either, suggesting the incomplete adaptation of vein graft and the inability of adult EC in gaining arterial identity in response to arterial hemodynamics [42,43]. In contrast, early stage ECs (*e.g.* embryonic stem cell derived ECs) are able to respond to hemodynamic stimuli by up-regulating arterial markers [44]. The data suggests that adult ECs gradually lose their phenotypic plasticity, and their arterial and venous identities are mostly determined by genetic factors rather than hemodynamics. Our data is in consistence with these findings. The differences in gene expression patterns of 2D vs. 3D are likely due to the matrix composition and stiffness that ECs reside on (collagen vs. plastic surface). This can also been reflected from the capillary morphogenesis within collagen matrix, which only occurred in the 3D static condition but not in the 3D flow condition, whereas this phenomena are not observed in both 2D static and 2D flow condition. These differences will also likely influence the gene expression patterns [45].

Generating a perfused vasculature is one of the most critical challenges in tissue engineering. Previously, several studies have used micro-fabrication technology to create precisely patterned microvascular channels seeded with ECs [46–49]. However, these microfluidic channels are made of plastic, PDMS or polymers, which do not allow native tissue remodeling between ECs and the surrounding matrix. Recently, a new development in this field has created perfused vascular structures with improved biological functions [50]. Using micro-patterned sacrificial materials, cells and collagen gel can form the vascular structure with the subsequent removal of the sacrificial materials [16,29,51]. Miller et al. developed a new method implementing the printed networks of carbohydrate glass, and used them as a sacrificial template in engineered tissues containing perfused vasculature [40]. Compare to these approaches, our 3D printing technology can generate perfused cell-gel structure using only cells and biological matrix, and is easy and straightforward. The 3D bio-printing technology allows simultaneous deposition of up to 8 different biomaterials. Multiple types of cells, scaffold precursors can be printed along with vasculature. The freeform fabrication does not require complicated steps of microfabrication and sample alignment, and can be easily adapted to create more sophisticated structures with multiple cell types and ECMS. For example, creating two channels with two different cell types or adding additional cell types into the matrix is relatively easy while it is difficult to achieve using other approaches. Creation of a vascular niche will also be possible using this technique; for example, neural stem cells can be embedded along with vasculatures and growth factors to examine how they mutually influence on network formation [52]. It also can be applied to develop an *in vitro* experimental model for hypoxia, tissue repair, and tumor angiogenesis research. In addition, investigations on the maturation process of engineered vasculature, capillary formation, and angiogenic sprouting will give insight into the EC behavior under 3D flow conditions, and increase our understanding on vascular biology. In addition, we can easily alter many factors related to vascular functions in this vascular channel model, such as the composition of vascular cells and supporting cells, flow rate/flow pattern, injection of soluble factors/small molecules, and other media components. Thus, the vascular channels can be served as an experimental model for diverse vascular disease-related studies such as inflammation, immune responses, and tumor angiogenesis.

5. Conclusion

In this study, we developed a functional *in vitro* vascular channel with perfused open lumen, the entire surface of which is fully covered with ECs, presenting barrier function for both plasma protein and dextran molecule. The fluidic vascular channel was capable to support the viability of tissue up to 5 mm in distance with 5 million cells/mL density under the physiological perfusion condition. In a static culture condition, active angiogenic invasion of cells was observed. Gene expression analysis was reported in this study to show the potential of the vascular channel in vascular biology research. The methods have great potential in vascularized tissue fabrication as the vascular channel is simultaneously created while cells and matrix are printed around the channel in desired 3D patterns. It can also serve as a unique experimental tool for investigating fundamental mechanisms of vascular function and maturation process under 3D flow conditions.

Acknowledgments

References

[1] Norotte C, Marga FS, Niklason LE, Forgacs G. Scaffold-free vascular tissue engineering using bioprinting. Biomaterials 2009;30:5910–7.

[2] Mironov V, Visconti RP, Kasyanov V, Forgacs G, Drake CJ, Markwald RR. Organ printing: tissue spheroids as building blocks. Biomaterials 2009;30:2164–74.

[3] Roth EA, Xu T, Das M, Gregory C, Hickman JJ, Boland T. Inkjet printing for high-throughput cell patterning. Biomaterials 2004;25:3707–15.

[4] Dhariwala B, Hunt E, Boland T. Rapid prototyping of tissue-engineering constructs, using photopolymerizable hydrogels and stereolithography. Tissue Eng 2004;10:1316–22.

[5] Landers R, Hübner U, Schmelzeisen R, Mülhaupt R. Rapid prototyping of scaffolds derived from thermoreversible hydrogels and tailored for applications in tissue engineering. Biomaterials 2002;23:4437–47.

[6] Liu Tsang V, Chen AA, Cho LM, Jadin KD, Sah RL, DeLong S, et al. Fabrication of 3D hepatic tissues by additive photopatterning of cellular hydrogels. FASEB J 2007;21:790–801.

[7] Jakab K, Neagu A, Mironov V, Markwald RR, Forgacs G. Engineering biological structures of prescribed shape using self-assembling multicellular systems. Proc Natl Acad Sci U S A 2004;101:2864–9.

[8] Mironov V, Reis N, Derby B. Review: bioprinting: a beginning. Tissue Eng 2006;12:631–4.

[9] Cui X, Boland T. Human microvasculature fabrication using thermal inkjet printing technology. Biomaterials 2009;30:6221–7.

[10] Lee V, Singh G, Trasatti JP, Bjornsson C, Xu X, Tran TN, et al. Design and fabrication of human skin by three-dimensional bioprinting. Tissue Eng Part C Methods 2014;20:473–84.

[11] Zhao L, Lee VK, Yoo S-S, Dai G, Intes X. The integration of 3D cell printing and mesoscopic fluorescence molecular tomography of vascular constructs within thick hydrogel scaffolds. Biomaterials 2012;33:5325–32.

[12] Lee W, Debasitis JC, Lee VK, Lee J-H, Fischer K, Edminster K, et al. Multi-layered culture of human skin fibroblasts and keratinocytes through three-dimensional freeform fabrication. Biomaterials 2009;30:1587–95.

[13] Langer RS, Vacanti JP. Tissue engineering: the challenges ahead. Sci Am 1999;280:86–9.

[14] Folkman J. Angiogenesis in cancer, vascular, rheumatoid and other disease. Nat Med 1995;1:27–31.

[15] Lee W, Lee V, Polio S, Keegan P, Lee J-H, Fischer K, et al. On-demand three-dimensional freeform fabrication of multi-layered hydrogel scaffold with fluidic channels. Biotechnol Bioeng 2010;105:1178–86.

[16] Chrobak KM, Potter DR, Tien J. Formation of perfused, functional microvascular tubes in vitro. Microvasc Res 2006;71:185–96.

[17] Golden AP, Tien J. Fabrication of microfluidic hydrogels using molded gelatin as a sacrificial element. Lab Chip 2007;7:720–5.

[18] Lee Y-B, Polio S, Lee W, Dai G, Menon L, Carroll RS, et al. Bio-printing of collagen and VEGF-releasing fibrin gel scaffolds for neural stem cell culture. Exp Neurol 2010;223:645–52.

[19] Ozturk MS, Lee VK, Zhao L, Dai G, Intes X. Mesoscopic fluorescence molecular tomography of reporter genes in bioprinted thick tissue. J Biomed Opt 2013;18:100501.

[20] Price GM, Tien J. Methods for forming human microvascular tubes in vitro and measuring their macromolecular permeability. Methods Mol Biol 2011;671: 281–93.

[21] Mehta D, Malik AB. Signaling mechanisms regulating endothelial permeability. Physiol Rev 2006;86:279–367.
[22] Dekker RJ, van Soest S, Fontijn RD, Salamanca S, de Groot PG, VanBavel E, et al. Prolonged fluid shear stress induces a distinct set of endothelial cell genes, most specifically lung Krüppel-like factor (KLF2). Blood 2002;100:1689–98.
[23] Parmar KM, Larman HB, Dai G, Zhang Y, Wang ET, Moorthy SN, et al. Integration of flow-dependent endothelial phenotypes by Kruppel-like factor 2. J Clin Invest 2006;116:49–58.
[24] Dai G, Kaazempur-Mofrad MR, Natarajan S, Zhang Y, Vaughn S, Blackman BR, et al. Distinct endothelial phenotypes evoked by arterial waveforms derived from atherosclerosis-susceptible and -resistant regions of human vasculature. Proc Natl Acad Sci U S A 2004;101:14871–6.
[25] Brooks AR, Lelkes PI, Rubanyi GM. Gene expression profiling of human aortic endothelial cells exposed to disturbed flow and steady laminar flow. Physiol Genomics 2002;9:27–41.
[26] Hahn C, Schwartz MA. Mechanotransduction in vascular physiology and atherogenesis. Nat Rev Mol Cell Biol 2009;10:53–62.
[27] Davis G, Stratman, Sacharidou A. Molecular control of vascular tube morphogenesis and stabilization: regulation by extracellular matrix, matrix metalloproteinases, and endothelial cell–pericyte interactions. Biophysical regulation of vascular differentiation and assembly. New York: Springer; 2011. pp. 17–47.
[28] Iruela-Arispe ML, Davis GE. Cellular and molecular mechanisms of vascular lumen formation. Dev Cell 2009;16:222–31.
[29] Nguyen DH, Stapleton SC, Yang MT, Cha SS, Choi CK, Galie PA, et al. Biomimetic model to reconstitute angiogenic sprouting morphogenesis in vitro. Proc Natl Acad Sci U S A 2013;110:6712–7.
[30] Koh W, Stratman AN, Sacharidou A, Davis GE. In vitro three dimensional collagen matrix models of endothelial lumen formation during vasculogenesis and angiogenesis. Methods Enzymol 2008;443:83–101.
[31] Nakatsu MN, Hughes CC. An optimized three-dimensional in vitro model for the analysis of angiogenesis. Methods Enzymol 2008;443:65–82.
[32] Yancopoulos GD, Davis S, Gale NW, Rudge JS, Wiegand SJ, Holash J. Vascular-specific growth factors and blood vessel formation. Nature 2000;407:242–8.
[33] Carmeliet P, Tessier-Lavigne M. Common mechanisms of nerve and blood vessel wiring. Nature 2005;436:193–200.
[34] Li Y-SJ, Haga JH, Chien S. Molecular basis of the effects of shear stress on vascular endothelial cells. J Biomech 2005;38:1949–71.
[35] Nakatsu MN, Sainson RCA, Aoto JN, Taylor KL, Aitkenhead M, Pérez-del-Pulgar S, et al. Angiogenic sprouting and capillary lumen formation modeled by human umbilical vein endothelial cells (HUVEC) in fibrin gels: the role of fibroblasts and angiopoietin-1. Microvasc Res 2003;66:102–12.
[36] Chen X, Aledia AS, Ghajar CM, Griffith CK, Putnam AJ, Hughes CCW, et al. Prevascularization of a fibrin-based tissue construct accelerates the formation of functional anastomosis with host vasculature. Tissue Eng Part A 2009;15: 1363–71.
[37] Hsu YH, Moya ML, Abiri P, Hughes CC, George SC, Lee AP. Full range physiological mass transport control in 3D tissue cultures. Lab Chip 2013;13:81–9.
[38] Komarova Y, Malik AB. Regulation of endothelial permeability via paracellular and transcellular transport pathways. Annu Rev Physiol 2010;72:463–93.
[39] Oh P, Borgstrom P, Witkiewicz H, Li Y, Borgstrom BJ, Chrastina A, et al. Live dynamic imaging of caveolae pumping targeted antibody rapidly and specifically across endothelium in the lung. Nat Biotechnol 2007;25:327–37.
[40] Miller JS, Stevens KR, Yang MT, Baker BM, Nguyen DH, Cohen DM, et al. Rapid casting of patterned vascular networks for perfusable engineered three-dimensional tissues. Nat Mater 2012;11:768–74.
[41] Nelson CM, Tien J. Microstructured extracellular matrices in tissue engineering and development. Curr Opin Biotechnol 2006;17:518–23.
[42] Kudo FA, Muto A, Maloney SP, Pimiento JM, Bergaya S, Fitzgerald TN, et al. Venous identity is lost but arterial identity is not gained during vein graft adaptation. Arterioscler Thromb Vasc Biol 2007;27:1562–71.
[43] Muto A, Yi T, Harrison KD, Davalos A, Fancher TT, Ziegler KR, et al. Eph-B4 prevents venous adaptive remodeling in the adult arterial environment. J Exp Med 2011;208:561–75.
[44] Masumura T, Yamamoto K, Shimizu N, Obi S, Ando J. Shear stress increases expression of the arterial endothelial marker ephrinB2 in murine ES cells via the VEGF-Notch signaling pathways. Arterioscler Thromb Vasc Biol 2009;29: 2125–31.
[45] Bell SE, Mavila A, Salazar R, Bayless KJ, Kanagala S, Maxwell SA, et al. Differential gene expression during capillary morphogenesis in 3D collagen matrices: regulated expression of genes involved in basement membrane matrix assembly, cell cycle progression, cellular differentiation and G-protein signaling. J Cell Sci 2001;114:2755–73.
[46] Borenstein JT, Tupper MM, Mack PJ, Weinberg EJ, Khalil AS, Hsiao J, et al. Functional endothelialized microvascular networks with circular cross-sections in a tissue culture substrate. Biomed Microdevices 2010;12:71–9.
[47] Shin M, Matsuda K, Ishii O, Terai H, Kaazempur-Mofrad M, Borenstein J, et al. Endothelialized networks with a vascular geometry in microfabricated poly(dimethyl siloxane). Biomed Microdevices 2004;6:269–78.
[48] King K, Wang C, Kaazempur-Mofrad M, Vacanti J, Borenstein J. Biodegradable microfluidics. Adv Mater 2004;16:2007–12.
[49] Bettinger C, Weinberg E, Kulig K, Vacanti J, Wang Y, Borenstein J, et al. Three-dimensional microfluidic tissue-engineering scaffolds using a flexible biodegradable polymer. Adv Mater 2006;18:165–9.
[50] Moya ML, Hsu YH, Lee AP, Hughes CC, George SC. In vitro perfused human capillary networks. Tissue Eng Part C Methods 2013;19:730–7.
[51] Zheng Y, Chen J, Craven M, Choi NW, Totorica S, Diaz-Santana A, et al. In vitro microvessels for the study of angiogenesis and thrombosis. Proc Natl Acad Sci U S A 2012;109:9342–7.
[52] Gilbertson RJ, Rich JN. Making a tumour's bed: glioblastoma stem cells and the vascular niche. Nat Rev Cancer 2007;7:733–6.